ОБЗОРЫ

M. HASHEMIAN[1] and H. POURGHASSEM[1]

AUTISM SPECTRUM DISORDERS DIAGNOSING BASED ON EEG ANALYSIS: A SURVEY

Autism spectrum disorders (ASD) are pervasive neurodevelopmental conditions characterized by impairments in reciprocal social interactions, communication skills, and stereotyped behavior. Since EEG recording and analysis is one of the fundamental tools in diagnosis and identifying disorders in neurophysiology, researchers strive to use the EEG signals for diagnosing of individuals with ASD. We found that studies on the ASD diagnosis using EEG techniques could be divided into two groups, where analysis was based on either comparison techniques or pattern recognition techniques. In this paper, we try to explain these two sets of algorithms along with their applied methods and results. Ultimately, evaluation measures of diagnosis algorithms are discussed.

Keywords: autism spectrum disorders (ASD), EEG, feature extraction, classification, ASD diagnosis algorithms.

INTRODUCTION

Autism spectrum disorders (ASD) are pervasive neurodevelopmental conditions characterized by impairments in reciprocal social interactions, communication skills, and stereotyped behavior [1]. The ASD are composed of five disorders: autism, pervasive development disorder-not otherwise specified (PDD-NOS), Asperger's syndrome (AS), childhood disintegrative disorder (CDD), and Rett's disorder (RD) [2, 3]. Different nations have emphasis to the studies of ASD differently. For example, developing countries have paid further less attention to the subject matter. Since, the major part of performed studies on ASD prevalence has been reported in North America and European countries [4]. According to a few scientific investigations, there has been a growing rate of ASDs in recent years. For example, it has been estimated that, in the United Kingdom, 157 of 10,000 primary school children have, on average, ASD [5]. Also, the prevalence rate of ASD among the British adults has been estimated as 98 of 10,000 [6]. Likewise, in a research performed in the United States, the prevalence rate of ASD among 8-year-old children was estimated as 90 of 10,000 [7]. During 1966 to 2008, the prevalence rates of autism, PDD-NOS, and AS were estimated 20, 30, and 2 of 10,000, respectively [8]. Based on a preliminary research, the prevalence rates for Iranian children were found to be 19 and 5 of 1,000 for autistic and AS disorders, respectively [9]. Moreover, in another study, the number of Iranian university students with ASD was revealed to be 120 of 1,000. Additionally, the number of males (as compared with that of females) was significantly higher [10].

The diagnosis of ASD is not an easy process and generally requires estimation of certain behavioral and cognitive characteristics [11]. Today, the researchers are trying to find the ASD diagnostic approaches through electrophysiological and neuroimaging techniques. Since EEG recording and analysis is one of fundamental tools in diagnosis and identifying disorders in neurophysiology, the researchers strive to use the EEG technique for diagnosing of individuals with ASD. A group of the studies have investigated that EEG signals of individuals with ASD are relevant to age- and intelligence quotient (IQ)-matched control subjects based on different conditions. In these studies, comparative methods and statistical criteria to analyze the results have been used. In became possible to identify some characteristics of the brain signals that explicitly differentiate between the EEG signals of normal individuals and individuals with ASD. However, it is noteworthy to mention that these studies

[1] Department of Electrical Engineering, Najafabad Branch, Islamic Azad University, Isfahan, Iran.
Correspondence should be addressed to H. Pourghassem
(e-mail: h_pourghasem@iaun.ac.ir).

have only sometimes provided identical results. The next group of studies has taken large steps in the path of diagnosing ASD by using pattern recognition and classification techniques that they have been able to separate the brain signal patterns of normal individuals from those affected with ASD. In other words, the consequences of studies provide high-performance diagnostic algorithms. Therefore, we found that the researches on brain signal processing of individuals with ASD could be divided into two groups where analysis was based either on comparison techniques or on pattern recognition techniques (Fig. 1). These two groups of studies represent developmental progress over the decade in the ASD detection.

In this paper, we try to present an overview of the recent researches on EEG-based diagnosis approached of ASD. Moreover, this overview provides a rather comprehensive outlook on the ASD. We divided the performed studies in ASD analysis into the two above-mentioned main groups. In each group, we describe the principle of presented algorithms, evaluation measures of ASD detection and diagnosis, and reported results. Moreover, we mention the strong and weak points of the algorithms presented in the literature.

ASD ANALYSIS BASED ON EEG COMPARISON TECHNIQUES

In the studies of ASD diagnosis based on comparison techniques, a comparison between the EEG signals of normal individuals to those affected with ASD in terms of their age and IQ is carried out. Two main factors are considered in the process of EEG signal comparison. Firstly, what types of characteristics are being examined? In the EEG signals, the valuable information needing to be extracted and compared has
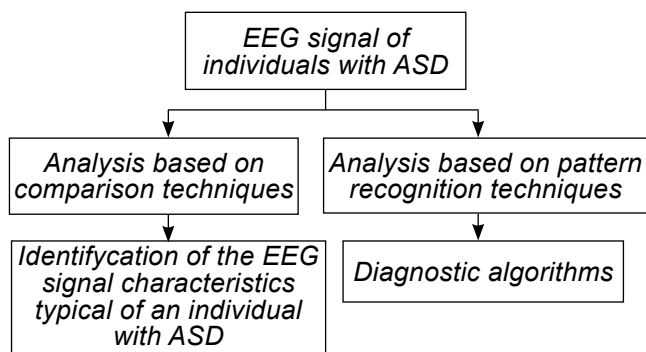

F i g. 1. Categorization of the reported researches.

Р и с. 1. Категоризація досліджень, представлених в огляді.

been concealed. The extracted information is called "features," and each one of these features is obtained by using various signal processing methods and different scenarios. Secondly, what statistical method should be used to measure the difference between the EEG ASD-related and non-ASD samples according to the characteristics?

In each study, an appropriate statistical method based on comparison models, examined factors, and related hypotheses is used for ASD detection. In majority of these statistical techniques, like analysis of variance (ANOVA) and the t-test, the result of compared process is denoted by index P (probability of the zero hypothesis). If the value of P is less than the preset significance level ($P <$ alpha), it represents a statistically significant difference in the evaluated characteristics of samples. In each process, the significance level is determined based on the acceptable error level. In most studies, values of 0.01 or 0.05 are considered for the alpha value. When the P value on only slightly greater than, e.g., 0.05, such a situation can be interpreted as the absence of a significant difference between the compared values but as a trend toward such a difference.

EEG SIGNAL FEATURES FOR ASD ANALYSIS

EEG Rhythms. In ASD analysis, EEG rhythms are the most common used features based on the comparison technique. The EEG rhythms according to their frequency bands are most commonly divided as follows. The delta rhythm corresponds to 2-4 Hz, theta rhythm, to 4-8 Hz, alpha rhythm and mu rhythm, to 8-13 Hz, beta rhythm, to 13-30 Hz, and gamma rhythm, to the frequencies higher than 30 Hz. In some studies, the proposed borders between the above ranges can be slightly (insignificantly) diferent. The EEG rhythms have a crucial role for perceiving brain functions. For example, it seems that working memory-related processes are marked as oscilations in the EEG theta frequencies [12-14]. Concerning the cognitive processes, three alpha subrhythms have recently been found, the lower-1 alpha (with 6-8 Hz oscilations) responding to cognitive processes named as "alertness," the lower-2 alpha (with 8-10 Hz fluctuations) that seems to be related with attentional demands [15], and, finally, upper alpha (with 10-12 Hz oscilations) that seems to be related with stimulus features and/or semantic processes of

memory [16-19].

The so-called mu rhythm is typically maximum over the sensorimotor cortex at the resting state and is attenuated by voluntary movements or somatosensory stimulation. This rhythm is slightly affected by visual stimulation. In other words, the mu rhythms suggest the presence of sensorimotor processing in frontoparietal networks. At the same time, the classical alpha rhythms suggest the initial visual processing in the occipital networks [20].

Desynchronization of the beta rhythm usually occurs during motor activities. The synchronization, however, occurs immediately after the movement (beta rhythm rebound) [21]. These processes represent the action of the motor cortices [22-25]. The reactions of the beta rhythm have been also recorded when observing other movements and during motor imagery. Additionally, the gamma band is observable at the existence of the visual and/or auditory motor tasks [26-31].

Absolute Power or Relative Power. The absolute spectral power (ASP) within a given frequency band corresponds to the area underneath of spectral curves for the respective frequency band. The relative spectral power (RSP) is a percentage value that compared the absolute power within a given frequency band to the total (integral) absolute power for the entire frequency range. In other words, the relative power, or the band relative intensity ratio (RIR), can be defined for each frequency band i as

$$RIR_i = \frac{absolute\ power_i}{\sum_i absolute\ power}\ ,\ i = \delta, \theta, \alpha, \beta,\ \text{and}\ \gamma \quad (1)$$

Coherence. Coherence is a benchmark of coupling between two different time series in the frequency domain. The estimated coherence can indicate the "coupling" of functional association between two brain regions [32]. The coherence between two EEG channels presents the linear relationship of these two channels at a specific frequency. Mathematically, the coherence is calculated as

$$Coh_{ij}(f) = \left| \frac{S_{ij}(f)}{(S_{ii}(f)S_{jj}(f))^{\frac{1}{2}}} \right| \quad (2)$$

$$S_{ij}(f) = \langle X_i(f)\, X_j^{*}(f) \rangle \quad (3)$$

where $X_i(f)$ and $X_j(f)$ are the (complex) Fourier transforms of time series $x_i(t)$ and $x_j(t)$ of channels i and j, respectively. $S_j(f)$ is the cross-spectrum function where operator "*" means complex conjugation, and $\langle \rangle$ means the expectation value. In practice, the expectation value can only be estimated as an average over a sufficiently large number of epochs [33]. The estimated coherence is a value within [0, 1] range. If the value of coherence function is calculated as zero (i.e., in the frequency f_o, $C_{ij}(f_o) = 0$), it indicates that the activities of signals in this frequency are linearly independent. At the same time, a value of one, i.e., $C_{ij}(f_o) = 1$, gives the maximum linear correlation for this frequency [34]. Figure 2 indicates a model of the applied analysis based on the coherence measure in two groups of children (ASD and non-ASD) [35]. According to this analysis, the dotted and solid lines, respectively, show the significant differences for $P < 0.05$ and $P < 0.01$ in terms of the coherence values for three frequency bands (gamma, alpha, and beta) between these two groups.
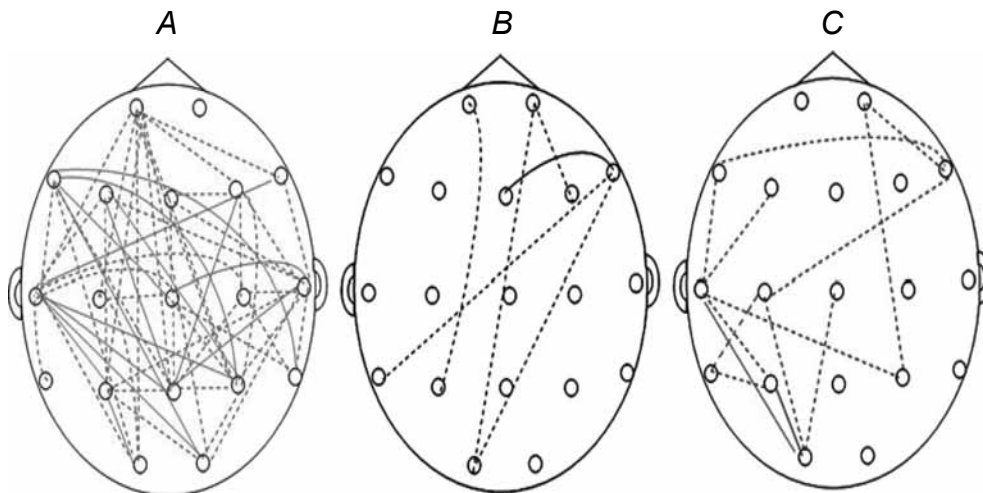

F i g. 2. A model of the applied analysis based on coherence measure [35] .

Р и с. 2. Модель прикладного аналізу, базована на оцінці когерентності [35].

Mu Wave Suppression. The properties of the mu frequency band can be used as a technique to investigate human mirror neuron functioning [36]. At the resting state, the synchronous action of the neurons in the sensorimotor cortex creates large mu oscillations. When individuals execute or observe a movement, the power of these mu oscillations is attenuated. This phenomenon is called mu wave suppression [36-39]. The amplitude reduction of mu oscillations indicates desynchronization of the underlying neurons, reflecting greater levels of active processing during motor movement and observation [38, 39].

Cordance. Cordance is a measurable EEG factor to determine the cerebral blood flow perfusion and metabolism. In fact, this factor is an incorporation of both relative and absolute power measures to produce characteristics that are more strongly correlated with local cerebral perfusion than each separate measure [40]. The cordance is calculated based on an algorithm consisting of three steps. Firstly, the values of EEG power are calculated by an arrangement of reattributional electrodes. The reattributed power is the average of power values from pairs of electrodes that share a common electrode. [41]. In the second step, the values of relative and absolute powers of each individual EEG recording are statistically standardized among the electrode sites, engaging a z-transformation for the each electrode site for corresponding frequency band *f*. According to this way, the values of $A_{norm}(s,f)$ and $R_{norm}(s,f)$ are determined. Finally, the values of cordance for each electrode site *s* and its corresponding frequency band *f* are determined by the following relation [42]:

$$Cordance_{(s,\,f)} = A_{norm\,(s,\,f)} + R_{norm\,(s,\,f)}$$

Multi-Scale Entropy. Multi-scale entropy (MSE) is a computational method for quantifying the complexity of a time series by calculating the sample entropy (S_F) over several time scales, with utilizing a coarse-graining procedure [43, 44]. The S_F is a measure of irregularity of a time-series in an EEG time-series $x = \{x_1,...x_i,...x_N\}$, defined as negative of the logarithmic conditional probability that two similar sequences of *m* consecutive data points will remain similar at the next point ($m + 1$) [45-47].

$$S_E(m, r, N) = -L_n(\frac{C_{m+1}(r)}{C_m(r)}) \qquad (5)$$

where $C_m(r) = \frac{A}{B}$, *A* is the number of pairs (*i, j*) with $|x_i^m - x_j^m| < r$, $i = j$, and *B* is the number of all probable pairs, $\frac{N-m+1}{N-m+1}$ where $|x_i^m - x_j^m| < r$ denotes the distance between vectors x_i^m and x_j^m with dimension *m*, *r* is the tolerable distance between two vectors (in terms of the standard deviation fraction of the time-series), and *N* is the length of time-series. For MSE analysis, the EEG time-series $x = \{x_1,...x_i,...x_N\}$ is coarse-grained into consecutive time-serie $\{y_j^\tau\}$ corresponding to the scale factor (SF) τ. Firstly, the original time-series is divided into non-overlapping windows of length τ, and then the data points inside each window are averaged. Therefore, each coarse-grained time-series is defined as

$$y_j^\tau = (\frac{1}{\tau}) \sum_{i=(j-1)\tau+1}^{j\tau} x_i \,, \; 1 \le j \le \frac{N}{\tau} \qquad (7)$$

Eventually, S_E is calculated for each time-series $\{y_j^\tau\}$ [47]. Figure 3 illustrates the diagram of the coarse-graining procedure [44].
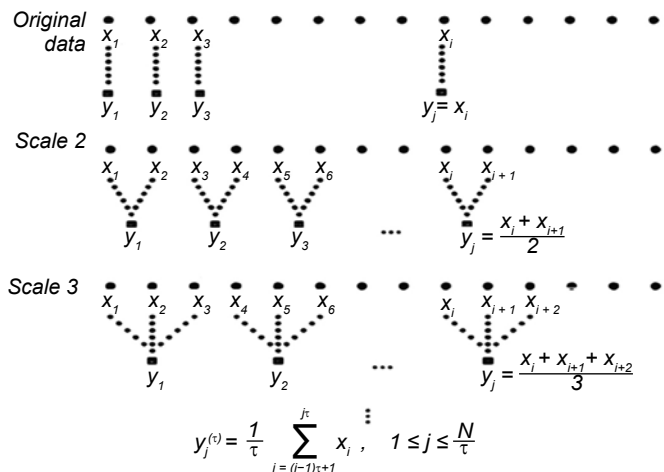
F i g. 3. Diagram of the coarse-graining procedure [44].

Р и с. 3. Діаграма процедури огрублення дискретизації [44].

ALGORITHMS BASED ON COMPARISON TECHNIQUES

The reported studies in the comparison-based algorithms could differ from each other regarding several views, including (i) age and IQ of the participants in each experiment, (ii) conditions under which the EEG signals have been registered, (iii) the features that have been extracted and compared

in both groups and in each experiment, and (iv) the factors that affect the results of every experiment. We briefly explain below the conditions and factors examined in each study along with their results for state-of-the-art studies that have been presented in the literature. For example, Daoust et al. [48] investigated EEGs of IQ-matched 9 persons with ASD (ages 12 to 53 years) and 8 control participants (ages 8 to 56 years) recorded under two conditions, REM sleep and wakefulness. In this study, the power spectral analysis was performed in four frequency bands: delta (0.75-3.5 Hz), theta (4.0-7.75 Hz), alpha (8.0-12.75 Hz), and beta (13.0-19.75 Hz). The report of these authors [48] indicated that individuals suffering from ASD, when being in REM sleep in comparison with the controls, demonstrated a significantly lower absolute beta spectral amplitude in primary (O1, O2) and associative (T5, T6) cortical visual areas. At the same time, subjects suffering from ASD, demonstrated significantly higher absolute theta spectral amplitudes in the left frontal pole region (Fp1) in the evening wakefulness, but not in the morning wakefulness [48]. In another study, Oberman et al. [49] recorded EEG signals from 10 high-functioning individuals of different ages (6-47 years) and gender with ASD and from matched control subjects in a parallel manner with watching videos of a moving hand or a bouncing ball, with moving their own hand, or against the background of visual noise. Then the mu-frequency power at scalp locations corresponding to sensorimotor cortex (C3, Cz, and C4) during the self-initiated action and watching action conditions was compared to the power under baseline (visual white noise) conditions. In other words, the mu wave suppression was estimated. Ultimately, the report revealed that mu suppression of self and observed hand movements in control participants was significant. Meanwhile, mu suppression of the participants with ASD in self-induced hand movements (but not in observed hand movements) was significant [49]. Stroganova et al. [50] recorded EEG signals from 44 boys with ASD (ages 3-8 years) and from a corresponding number of age-matched typically developing boys under conditions including sustained visual attention (presentation of soap bubbles or computer presentation of a moving fish). Then, the authors evaluated the EEG spectral power (SP) and SP interhemispheric asymmetry within delta, theta, and alpha bands in both groups. The researchers concluded that boys suffering from ASD were in fact a heterogeneous group with regard

to the alpha and theta SPs. The group yielded a high intergroup difference in absolute SPs of the prefrontal delta. The left-side broadband EEG asymmetry in such children was not typical, and the mid-temporal regions had the maximum intensity in this regard [50].

Murias et al. [51] investigated EEG measures in 18 male adults with ASD and 18 control male subjects (18-38 years old) in the resting state with the eyes closed. The coherence between pairs of electrodes and the relative SPs were evaluated. For the ASD group, locally higher coherence was clear within the theta frequency range (3-6 Hz). This was specifically evident in the temporal and frontal regions of the left hemisphere. For the lower alpha range (8-10 Hz), there was generally reduced coherence for the ASD group in the frontal regions and also between the frontal and all other scalp regions. In the ASD group, the relative SPs of the ranges between 3-6 and 13-17 Hz were significantly higher, but this parameter was significantly lower for 9-10 Hz [51].

Moreover, Bernier et al. [52] examined EEGs of 18 high-functioning adults with ASD and 15 IQ- and age-matched typical subjects participated in four conditions (resting, observation, execution, and imitate). The EEG mu rhythm was compared between two groups. The experiments illustrated that, with executing an action, both groups exhibited significant attenuation of the mu rhythm. When observing a movement, however, considerably reduced attenuation of the mu waves was observed in the ASD subjects [52]. In another study, Orekhova et al. [53] recorded EEGs in two independent samples of 3- to 8-year old boys with autism (BWA) from Moscow (20 boys) and Gothenburg (20 boys), and in the same number of age-matched typically developing boys (TDB) during sustained visual attention. The mean ASPs were calculated for three high-frequency bands, beta (13.2-24 Hz), gamma 1 (24.4-44.0 Hz), and gamma 2 (56.0-70 Hz). The authors reported that, a pathological rise was observed in the gamma intensity (24.4-44.0 Hz) in both BWA samples. Also, there was positive correlation between the intensity of gamma activity and the developmental delay rate in both BWA subgroups [53]. Coben et al. [54] investigated the EEG measures under eyes-closed resting conditions in 20 children diagnosed with ASD and 20 controls matched for gender, age (6-11 years old), and IQ. The ASPs, RSPs, and total SPs, as well as intrahemispheric and interhemispheric coherences, were calculated for these two groups. It was found that children with ASD noticeably differed in terms of the power and inter-

intrahemispheric coherences. In autistic children, an excess theta-RSP appeared especially in the posterior regions of the right hemisphere. Meanwhile, the delta SP in the frontal cortex was rather low, but the midline beta power was high. In the frontal regions of both hemispheres, theta and delta coherences were rather small. In addition, theta, delta, and alpha hypocoherences were observable in the temporal regions. Finally, theta, delta, and beta coherences were rather weak in the posterior regions [54].

Martineau et al. [55] compared EEG activity in 14 right-handed children with ASD and 14 right handed, age- and gender-matched control children (3 girls and 11 boys aged 5 years 3 months to 7 years 11 months) in the movie watching state. The silent movie consisted of four sequences, namely (i) no stimulation, "white" (Wh, TV screen white), (ii) a no movement sequence, "lake" (Lk, a body of water surrounded by land), (iii) a non-human movement sequence, "waterfall" (Wf, falling water), and (iv) a human movement sequence, "rotating" (Ro, a woman performing scissor movements with her legs while lying on her back). In this research, the logarithm absolute spectral power (Ln ASP) in each of the three following frequency bands, theta 1 (3-5.5 Hz), theta 2 (5.5-7.5Hz), and alpha 1 (7.5-10.5 Hz), were calculated. In was reported that, during observation of human actions in the normal children group, EEG desynchronization was observable in the frontal and temporal cortices and in the motor cortex areas. However, such a desynchronization was not evident in ASD children [55].

Raymaekers et al. [36] investigated the mirror neuron functioning. The EEG signals were recorded from 20 children with high-functioning autism (HFA, ages 8-13 years) and a control group of 19 typically developing age-matched children. The testing was based on the paradigm of Oberman et al. [49] consisted of four conditions, (i) observing a video of a moving hand (hand), (ii) moving own hand (self), (iii) watching a video of two bouncing balls (balls), and (iv) watching visual white noise (baseline). The mu wave suppression was calculated as a ratio of 8-13 Hz SP during each of the self, hand, and balls conditions relative to the respective power under baseline conditions. The report indicated that significant mu suppression in both self and observed hand movements were evident in both groups [36]. In the same year, Lazarev et al. [56] investigated the EEG photic driving at various stimulation frequencies (intermittent photic stimulation at 11 fixed frequencies, from 3 to 24 sec^{-1}

in 14 autistic boys (6-14 years old) and 21 control boys matched in age. The interhemispheric asymmetry in the total number of driving peaks in each group and the difference between autistic and control groups in each hemisphere were evaluated for each frequency band of the four harmonics in the non-visual areas and the sum of four harmonics in both non-visual and occipital visual areas. The researchers deduced that boys with autism showed latency abnormalities in the right hemisphere during the photic driving reactivity, particularly at the rapid alpha and beta frequencies of stimulation [56].

Thatcher et al. [57] recorded EEG from 54 autistic subjects and 241 normal subjects (2.6 to 11 years old) under resting conditions with the eyes open. The EEG phase shift and phase lock durations were computed for all possible electrode combinations; two alpha (8-10 and 10-13 Hz and three beta subranges 13-15, 15-18, and 25-30 Hz) were considered. It was recognized that the phase shift duration in ASD children in both short (6 cm) and long (21-24 cm) interelectrode distances in all bands of frequency, particularly in the alpha1 frequency band (8-10 Hz), was significantly shorter [57]. Chan et al. [58] investigated EEGs of 38 normal children and 16 children with ASD (6-14 years old) that were recorded under the eyes-open condition. Cordance was computed for 19 electrode sites using a three-step algorithm [44, 46] as a feature. The obtained results also demonstrated that cordance patterns of the ASD subjects were lower as compared with those of normal ones, possibly indicating that perfusion within the frontal regions of ASD subjects is lower than that in normal ones [58].

Lazarev et al. [59] examined photic driving coherence during intermittent photic stimulation in 14 autistic boys (6-14 years old, with IQ 91.4 ± 22.8) and 19 normally developing boys who were subjected to stimulation of 12 fixed frequencies (3 to 27 sec^{-1}). The number of high-coherent connections (HCC) (coherence > 0.6-0.8) was estimated among seven leads in each hemisphere. The findings showed that, unlike the spectral characteristics indicating deficit in the photic driving reactivity in the right hemisphere, the groups were different in terms of the number of HCC only in the left hemisphere. Also, there was increased prevalence of the frequency in the left hemisphere [59]. In the same year, Sudirman et al. [60] collected EEGs from 6 normal children, 2 autism-suffering children, and 8 Down syndrome children under the actions of two stimulus consisting of alternating checkerboard and ripple checkerboard.

The amplitudes of alpha frequency oscillations were compared in the above three groups. It was found that the alpha value for normal children, in comparison with Down syndrome and autistic children, was higher at 10 Hz [60].

Isler et al. [61] compared EEG activity in 6 children with ASD and 8 age- and gender-matched control children (5.5-8.5 years old) under visual stimulation (long-latency flash-evoked visual potentials). The EEG power and synchrony measures (coherence and phase synchrony) were computed. In autistic children, as compared with normal ones, the interhemisphere synchrony demonstrated a 50% reduction in the theta band. Also, the synchrony between the hemispheres in autistic subjects was not distinguishable above the theta band (uncorrelated cortical activity). In spite of a power bilateral increase, the synchrony between the hemispheres mitigated in autistic children. The wavelet power in children with autism had a more sluggish recovery, a faster primary reaction to stimulation, and a more modularity state at longer latencies. Catarino et al. [47], however, assessed EEGs in 15 participants with ASD (23.79-42.34 years old) and 15 typical controls (21.50-37.77 years old) under a face and chair matching task (stimuli consisted of 30 pictures of neutral faces and 30 pictures of chairs.) The multiscale entropy and RSPs were compared in two groups. It was found that, in ASD children as compared to the control group, the EEG signal complexity was lower in the occipital and temporo-parietal areas. There was no significant variation between the groups in terms of the EEG power spectra [47]. In the same year, Chan et al. [62] studied EEGs of 21 children with ASD and 21 children with normal development (5-14 years old) facing the object recognition task (consisted of 24 line drawings taken from the object database by Snodgrass et al. [63] and modified/validated by Rossion et al. [64]). The line drawings were placed in an array of six by four layouts displayed on a computer screen for 3 min. The participants were required to memorize the items for a later recognition task (consisting of 12 targets mixed with 12 distracters). In this research, theta coherence measures (4-7.5 Hz) were used to evaluate and analyze EEG signals. The authors [62] deduced that ASD children, in comparison with normal ones, demonstrated a dissimilar pattern of EEG coherence.

In 2012, two studies related to ASG/EEG were published. Firstly, Lushchekina et al. [65] studied EEGs in 5- to 7-year-old children, both normal and with early childhood autism, under two resting conditions and at a cognitive task. The SPs and mean coherence for the alpha, beta, and gamma rhythms were compared. It was mentioned that, for both ASD and normal children, a frontal-occipital alpha gradient was considerable. For normal children, the SP and coherence of EEG rapid rhythms were significantly enhanced in the frontal and central regions of the left hemisphere under conditions of the cognitive tasks compared with the baseline ones [65]. Secondly, Mathewson et al. [66] investigated EEGs in 15 adults with ASD (18.8-51.6 years old) and a matched comparison group of 16 unimpaired adults (22.6-47.8 years old) under eyes-closed and eyes-open conditions. The EEG alpha SPs and coherence were computed for assessing the participants. Calculations showed that there was a difference between two groups in terms of coherence or eyes-closed EEG alpha SP. However, alpha suppression for eyes-open conditions was weaker in ASD adults, as compared with normal ones.

ASD ANALYSIS BASED ON PATTERN RECOGNITION TECHNIQUES

It has taken a giant leap in the direction of diagnosing ASD based on EEG analysis. The researches have used pattern recognition techniques to separate ASD and non-ASD brain signal patterns. Figure 4 illustrates a general structure of the ASD diagnosis algorithms based on the above-mentioned techniques. These algorithms consist of two main components, feature extraction and feature classification. The most commonly utilized tools and approaches in these algorithms are described below in detail.

Feature Extraction. The feature extraction stage can be considered as a mapping from the initial signal space to the feature space in a way that the separability may be improved in the new space. Different features
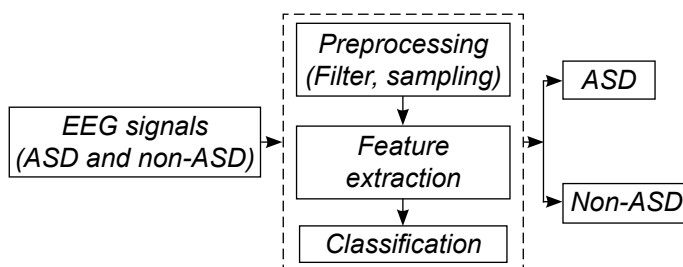

F i g. 4. General structure of diagnostic algorithms based on pattern recognition techniques.

Р и с. 4. Загальна структура діагностичних алгоритмів, що базуються на техніці розпізнавання образів.

The Employed Features of EEG Signals in the Frequency and Time Domains

Частотні та часові характеристики ЕЕГ-сигналів, застосовані для аналізу

Frequency/time domains	Description
Frequency domain	Short-Time Fourier Transform at a bandwidth (STFT-BW) in the total spectrum [68] STFT-BW component in the alpha band [69] Averaged values of the spectrogram greater than 70% maximum in the alpha frequency band [70],[35] Principle Components Analysis (PCA) to Short-Time Fourier Transform [74] Gaussian mixture model (GMM) in frequency domain [72] Katz's Fractal Dimensions in delta and gamma EEG sub-bands [71] Principal Components Analysis (PCA) of the coherence data [75] The raw data and Fast Fourier Transform (FFT) [76]
Time domain	Modified multi-scale entropy (mMSE) [73]

are extracted by certain methods and scenarios from the EEG signals. Eventually, the extracted features form a vector that is called the "feature vector." The feature vectors of samples are used in the classification stage. Table 1 exhibits the effective features that were extracted from the frequency and time domains of EEG signals in the ASD diagnosis algorithms.

Classification. Classification is the process of assigning a feature vector to one of predefined classes or categories in a manner that minimizes the error of classification [67]. In the ASD detection problem, two classes are individuals with ASD (class one) and those with no ASD (class two). This process is usually done by applying classifiers on the feature vectors of two classes. The essential part of this process is to know how a classifier assigns one of the two classes to an unknown feature vector. Almost all of the classifiers have a training phase by a specific algorithm, and then they become capable of classifying the samples. In actuality, the above-mentioned specific algorithms use feature vectors that have previously been extracted from EEG signals of both groups. There are varieties of classifiers, like an artificial neural network, support vector machine (SVM), statistical classifier, *K*-Nearest Neighbor (KNN), Linear Discriminant Analysis (LDA), and Quadratic Discriminant Analysis (QDA). In fact, each one of them has its own strategy. Parameter setting to each classifier would have a direct impact on its performance. We could easily see the significance of feature extraction process in the diagnostic algorithms because the input of classifiers is formed by feature vectors.

Algorithms Based on Pattern Recognition Techniques. In this section, we would like to describe the algorithms based on pattern recognition techniques provided by the researchers in the ASD detection.

Here, we have tried to bring up important factors in each algorithm, including the extracted features, the methods employed, the type of utilized classifier, and that of database. The database implies the EEG signals of ASD and non-ASD individuals, which have been used in the process of designing and evaluating the algorithm. Each database has its own parameters, such as conditions of EEG recording, the number of ASD and non-ASD people, their age range, and their IQ. For example, Sheikhani et al. [68] used EEG samples of 11 patients (9.2 ± 1.4 years old) and 10 control age-matched subjects under eye-opened conditions. The Lempel-Ziv (LZ) complexity, Short Time Fourier Transform (STFT), and STFT at a bandwidth (STFT-BW) in the total spectrum were extracted from EEG signals and then evaluated by the ANOVA test. Finally, the STFT-BW feature obtained the most difference between these two groups on the basis of ANOVA. In this study, the KNN classifier has been used to classify a feature vector. This algorithm has obtained 81.0% discrimination between normal and autism subjects with Mahalanobis distance [68]. In another study, Behnam et al. [69] utilized EEG signals of 10 ASD (6-11 years old) and 9 age-matched control subjects, which were collected under eye-opened conditions. The STFT-BW component in the alpha band (8-12 Hz) was calculated as a feature, and a KNN classifier with Mahalanobis distance was used. Eventually, this algorithm was able to separate the normal peoples from ASD ones with the accuracy rate of 89.5%. In this study, moreover providing diagnostic algorithm, the coherence measures between all 171 pairs of 19 channels in three frequency bands (alpha, beta, and gamma) of EEG were examined. The authors declared that there are more abnormalities in the connectivity between the left hemisphere and right

temporal lobe, as compared with other regions [69].

Sheikhani et al. [70] utilized qEEG of 15 children with Asperger disorder (10 boys and 5 girls, age 6-11 years) and 11 normal children (7 boys and 4 girls of the same age range). The EEG signals of two groups of subjects were recorded under nine conditions, including the eye-closed state, relaxed eye-opened condition, looking at three samples of the Kanizsa puzzle, looking at a mother's picture upright and inverted, and looking at a stranger's picture upright and inverted. The average spectrogram values greater than 70% of the maximum were employed as a discriminating feature on quantitative EEG signals in the frequency bands of delta (0-4 Hz), theta (4-8 Hz), alpha (8-12 Hz), beta (12-36 Hz), and gamma (36-44 Hz). For classification of ASD children *vs* normal children, a KNN classifier with Mahalanobis distance was utilized. Experimental results showed that the recorded signals under relaxed open-eyed conditions in the gamma band, those recorded with looking at a stranger's inverted-condition picture in the alpha and beta bands, and the ones obtained with participants looking at a mother's inverted picture in the beta band provided the best discriminations with the accuracy rate of 96.2, 83.3, 70.6, and 77.8%, respectively [70]. In the next year, Sheikhani et al. [35] gathered qEEG signals from 17 children (13 boys and 4 girls, 6 to 11 years) with ASD and 11 control children (7 boys and 4 girls of the same age range) under relaxed eye-opened conditions. Average values of the spectrogram (STFT) greater than 70% maximum (spectrogram criteria) were calculated from quantitative EEG signals in the delta, theta, alpha, beta, and gamma frequency bands. Among the obtained amounts in each frequency band, average values of the spectrogram in the alpha band showed the maximum difference between two groups, and such value was chosen as a feature. Finally, this algorithm was able to differentiate sick and healthy (control group) individuals with the accuracy rate of 96.4% [35].

Ahmadlou et al. [71] collected EEG signals from 9 ASD children (6 to 13 years old, average age of 10.8 years), and 8 non-ASD children (7 to 13 years old, average age of 11.2 years) under resting eye-closed conditions. Then, the Higuchi's fractal dimension (FD) and Katz's fractal dimension were computed in all EEG subranges produced by the wavelet decomposition, as well as in the entire band-limited EEG. Significant FDs in different loci and different EEG subranges or band-limited EEG for distinguishing ASD children from non-ASD children were determined by ANOVA. Finally, three characteristics, including Katz's fractal dimensions in delta (of loci Fp2 and C3) and gamma (of locus T6) EEG sub-bands, were chosen among the extracted features by ANOVA. The EEG data are classified into ASD and non-ASD children groups using the radial basis function classifier (RBFNN). This classifier yielded the accuracy rate of 90.0% for diagnosis of the ASD in the three-dimensional feature space [71].

In 2011, two main studies were reported. Firstly, Razali et al. [72] used EEG signals from 6 autistic and 6 control children (each group with the age around 7 to 9 years old) under conditions of a motor imitation task (to clinch their hand according to the video stimuli). A Gaussian mixture model was used as a method of feature extraction for analyzing the brain signals in the frequency domain. Then, the extraction data were classified using Multilayer Perceptron (MLP). This algorithm acquired 86.62% discrimination between two groups [72]. Secondly, Bosl et al. [73] collected an EEG database from 79 different infants (46 high ASD-risk infants, HRA, and 33 controls of five age groups, 6, 9, 12, 18, and 24 months) under resting state conditions. Modified Multi-scale Entropy (mMSE) was extracted as a feature vector. To obtain the best classification, the authors examined operations of three types of classifiers, including KNN, Bayes, and SVM. The differences appeared to be the greatest at ages of 9 to 12 months. In a nutshell, infants were classified with an over-80% accuracy into control and HRA groups at the age of 9 months. The classification accuracy for boys was close to 100% and remained high (70 to 90%) at the ages of 12 and 18 months. For girls, the classification accuracy was highest at the age of 6 months but declined thereafter [73].

Khazaal Shams et al. [74] collected EEG signals from six autistic children and six typical preschool subjects (around 7 to 9 years old) under two conditions in the open-eyed state and motor task movement (asked to follow the right and left hand movement movie). The feature extraction was performed by Principle Components Analysis (PCA) to STFT of the EEG signals. Then, MLP is used to classify the feature vectors. The results showed that the proposed algorithm gives the accuracy rate of 90-100% for autism and normal children in the motor task and around 90% in the detection of normal subjects in the open-eyed task [74].

In another study, Duffy et al. [75] gathered EEG data from 463 children who were diagnosed with ASD and from 571children considered neurotypical controls,

with ages ranging from 1 to 18 years, in the awake and alert state. The spectral coherence was calculated; then PCA of the coherence data was employed as an objective technique to reduce the variable number meaningfully. For 2- to 12-year-old children, 40 factors of PCA showed highly significant intergroup differences ($P < 0.0001$). Discriminant function analysis (DFA) was used for classification that yielded precision of 88.5% for the control subjects and precision of 86.0% for the individuals with ASD [75]. Alhaddad et al. [76] gathered EEG samples from eight children with ASD (5 boys and 3 girls, 10-11 years old) and four control children (all of them were boys, 10-11 years old) under a relaxed condition. The authors investigated different preprocessing techniques, such as referencing, filtering, windsorizing, and scaling, for obtaining the best classification accuracy. After preprocessing, the raw data and FFT were used as features. Finally, the extracted features were classified using Fisher Linear Discriminant Analysis (FLDA). It was reported that, among the applied preprocessing techniques, the Windsor-filtered data gave the best performance for both raw data (89.97 ± .02%) and FFT features (91.64 ± .021%) [76].

Evaluation Measures of the Diagnosis Algorithm. As was previously mentioned, the designed classifier in the diagnosis algorithms is trained by a dataset, and then the trained classifier is able to assign any unknown sample to either ASD class or non-ASD class. In the reality, after the design of an algorithm, it will be examined by a test dataset having samples of the ASD and non-ASD individuals already diagnosed by physicians. Now, the EEG signals of the individuals enter the algorithm (after preprocessing and feature extraction), and eventually the algorithm assigns one of the two labels (ASD and non-ASD) to the EEG signal. If the output of algorithm matched the findings of physicians, the sample has been classified correctly. In other words, the algorithm performance is calculated as the number of test samples identified correctly by the algorithm to the total number of the test dataset. Based on the above finding, an important question comes to mind: On what size of the test dataset the performance of the algorithm is based? In fact, the size of the test dataset should be large enough until the used classifier can generalize the unknown samples. It seems that the bigger size of the test dataset causes the higher validation of the performance. In other words, the algorithm enjoys higher generalization. However, due to the limitations of collecting the test dataset, the latter is usually rather small in most researches. Now,

another question may be raised: How we can achieve a high generalization algorithm in a limited test dataset? The cross-validation methods are the answer to this question. By using these methods in designing diagnostic algorithm, a highly reliable performance could be obtained despite of small database. Some of these methods are random subsampling, k-fold, and leave one-out. Some researchers have used these methods in their proposed ASD diagnostic algorithms.

CONCLUSION

We proposed a surway of the studies on ASD diagnosis algorithms based on EEG analysis. We found that the studies could be divided into two groups, analysis based on comparison techniques and analysis based on pattern recognition techniques. Analysis based on comparison techniques has been able to identify, by using statistical methods, some of the features of EEG, which were different in the ASD and non-ASD individuals. Through reviewing the data of the studies, we found that the results of these studies are dissimilar. Analysis based on pattern recognition techniques takes a big step in diagnosing ASD based on EEG signals. In such studies, the researchers were able to take the advantage of pattern recognition techniques to differentiate the brain signal patterns affected by ASD from those of non-ASD ones. The feature extraction and classification are two main components in the structure of all these algorithms. In the feature extraction phase, various features with different scenarios are extracted from EEG signals. Among all extracted features, the ones that highlight the greatest difference between two groups are selected and used in designing the algorithm. Eventually, the classifiers assign a label of either ASD or non-ASD to the EEG signals by using the extracted features. Each one of the diagnostic algorithms reports a performance based on a test dataset. It should be noted that the degree of generalization and validity of a diagnostic algorithm depend on two factors, the size of the used test dataset and the type of utilized cross-validation methods.

М. Хашемян[1], Х. Пургассем[1]

ДІАГНОСТИКА РОЗЛАДІВ АУТИСТИЧНОГО СПЕКТРА, ЩО ҐРУНТУЄТЬСЯ НА АНАЛІЗІ ЕЕГ (огляд)

[1] Наджафабадський підрозділ Ісламського університету Азад, Ісфаган (Іран).

Р е з ю м е

Розлади аутистичного спектра (autism spectrum disorders – ASD) – це глибокі відхилення розвитку нервової сфери, що характеризуються порушенням соціальних взаємодій, комунікативних навичок та стереотипної поведінки. Оскільки реєстрація та аналіз ЕЕГ є одними із фундаментальних засобів діагностики та ідентифікації нейрофізіологічних розладів, дослідники намагаються використовувати ЕЕГ-сигнали для діагностики ASD у тих або інших осіб. Як ми встановили, дослідження, спрямовані на діагностику ASD із застосуванням ЕЕГ-методик, можуть бути поділені на дві групи, коли аналіз базується або на техніці порівнянь, або на техніці розпізнавання образів. У цьому огляді ми намагались описати застосування двох відповідних комплексів алгоритмів, а також методики їх використання та отримані результати. Нарешті, обговорюється порівняльна ефективність вказаних алгоритмів діагностування.

REFERENCES

1. J. L. Matson and J. A. Boisijoli, "Strategies for assessing Asperger's syndrome: A critical review of data based methods," *Res. Autism Spectr. Disord.*, **2**, No. 2, 237-248 (2008).

2. J. L. Matson and N. F. Minshawi, *Early Intervention for Autism Spectrum Disorders: A Critical Analysis*, Elsevier Sci. Inc., Oxford (2006).

3. M. Hashemian and H. Pourghassem, "Facial emotion processing in autism spectrum disorder based on spectral features of EEG signals," *Int. J. Imaging Robotics*, **11**, No. 3, 68-80 (2013).

4. C. M. Zaroff and S. Y. Uhm, "Prevalence of autism spectrum disorders and influence of country of measurement and ethnicity," *Soc. Psychiat. Psychiatr. Epidemiol.*, **47**, No. 3, 395-398 (2012).

5. S. Baron-Cohen, F. J. Scott, C. Allison, et al., "Prevalence of autism-spectrum conditions: UK school-based population study," *Br. J. Psychiat.*, **194**, No. 6, 500-509 (2009).

6. T. S. Brugha, S. McManus, J. Bankart, et al., "Epidemiology of autism spectrum disorders in adults in the community in England," *Arch. Gen. Psychiat.*, **68**, No. 5, 459-465 (2011).

7. B. Mulvihill, M. Wintage, R. S. Kiby, et al., "Prevalence of autism spectrum disorders – Autism and Developmental Disabilities Monitoring Network, United States, 2006," *MMWR Surveill Summ.*, **58**, No. 10, 1-20 (2009).

8. E. Fombonne, "Epidemiology of pervasive developmental disorders," *Pediat. Res.*, **65**, No. 6, 591-598 (2009).

9. A. Ghanizadeh, "A preliminary study on screening prevalence of pervasive developmental disorder in school children in Iran," *J. Autism. Dev. Disord.*, **38**, No. 4, 759-763 (2008).

10. A. A. Nejatisafa, M.R. Kazemi, and J. Alaghebandrad, "Autistic features in adult population: evidence for continuity of autistic symptoms with normality," *Adv. Cognitive Sci.*, **5**, No. 3, 34-39 (2003).

11. M. Othman and A. Wahab, "Affective face processing analysis in autism using electroencephalogram," in: *Proceedings of the International Conference on Information and Communication Technology for the Muslim World (ICT4M) (December 13-14, 2010)*, Jakarta (2010).

12. W. Klimesch, "EEG alpha and theta oscillations reflect cognitive and memory performance: a review and analysis," *Brain Res. Brain Res. Rev.*, **29**, Nos. 2/3, 169-195 (1999).

13. S. Nasehi and H. Pourghassem, "Online mental task classification based on DWT-PCA features and probabilistic neural network," *Int. J. Imaging Robotics*, **7**, No. 1, 110-118 (2012).

14. S. Nasehi and H. Pourghassem, "A novel fast epileptic seizure onset detection algorithm using general tensor discriminant analysis," *J. Clin. Neurophysiol.*, **30**, No. 4, 362-370 (2013).

15. W. Klimesch, G. Pfurtscheller, and H. Schimke, "Pre- and post-stimulus processes in category judgement tasks as measured by event-related desynchronization (ERD)," *J. Psychophysiol.*, **6**, 185-203 (1992).

16. W. Klimesch, "Memory processes, brain oscillations and EEG synchronization," *Int. J. Psychophysiol.*, **24**, Nos. 1/2, 61-100 (1996).

17. W. Klimesch, H. Schimke, and J. Schwaiger, "Episodic and semantic memory: An analysis in the EEG theta and alpha band," *Electroencephalogr. Clin. Neurophysiol.*, **91**, No. 6, 428-441 (1994).

18. S. Nasehi and H. Pourghassem, "Automatic prediction of epileptic seizure using kernel fisher discriminant classifiers," in: *Proceeding of the International Conference on Intelligent Computation and Bio-Medical Instrumentation (ICBMI), (14-17 Dec. 2011)*, Wuhan, China (2011), pp. 200-203.

19. W. Klimesch, M. Doppelmayr, D. Rohm, et al., "Simultaneous desynchronization and synchronization of different alpha responses in the human electroencephalograph: a neglected paradox," *Neurosci. Lett.*, **284**, Nos. 1/2, 97-100 (2000).

20. J. A. Pineda, "The functional significance of mu rhythms: Translating 'seeing' and 'hearing' into 'doing'," *Brain Res. Rev.*, **50**, No. 1, 57-68 (2005).

21. S. Salenius, A. Schnitzler, R. Salmelin, et al., "Modulation of human cortical rolandic rhythms during natural sensorimotor tasks," *NeuroImage*, **5**, No. 3, 221-228 (1997).

22. R. Hari, R. Salmelin, J. P. Mäkelä, et al., "Magnetoencephalographic cortical rhythms," *Int. J. Psychophysiol.*, **26**, Nos. 1/3, 51-62 (1997).

23. G. Pfurtscheller, "Central beta rhythm during sensorimotor activities in man," *Electroencephalogr. Clin. Neurophysiol.*, **51**, No. 3, 253-264 (1981).

24. G. Pfurtscheller, A. Stancak, and C. Neuper, "Post-movement beta synchronization. A correlate of an idling motor area," *Electroencephalogr. Clin. Neurophysiol.*, **98**, No. 4, 281-293 (1996).

25. G. Pfurtscheller, K. Zalaudek, and C. Neuper, "Event-related beta synchronization after wrist, finger and thumb move-ment," *Electroencephalogr. Clin. Neurophysiol.*, **109**, No. 2, 154-160 (1998).

26. E. Basar, C. Basar-Eroglu, S. Karakas, et al., "Brain oscillations in perception and memory," *Int. J. Psychophysiol.*, **35**, Nos. 2/3, 95-124 (2000).

27. C. Tallon-Baudry, O. Bertrand, C. Delpuech, et al., "Stimulus specificity of phase-locked and non-phase-locked 40 Hz visual responses in human," *J. Neurosci.*, **16**, No. 13, 4240-4249 (1996).

28. C. Tallon-Baudry, O. Bertrand, C. Wienbruch, et al., "Combined EEG and MEG recordings of visual 40 Hz responses to illusory triangles in human," *NeuroReport*, **8**, No. 5, 1103-1107 (1997).

29. C. Tallon-Baudry, O. Bertrand, F. Peronnet, et al., "Induced gamma-band activity during the delay of a visual short- term memory task in humans," *J. Neurosci.*, **18**, No. 11, 4244-4254 (1998).

30. C. M. Krause, P. Korpilahti, B. Porn, et al., "Automatic auditory word perception as measured by 40 Hz EEG responses," *Electroencephalogr. Clin. Neurophysiol.*, **107**, No. 2, 84-87 (1998).

31. N. E. Crone, D. L. Miglioretti, B. Gordon, et al., "Functional mapping of human sensorimotor cortex with electrocorticographic spectral analysis. II. Event-related synchronization in the gamma band," *Brain*, **121**, No. 12, 2301-2315 (1998)

32. P. L. Nunez, R. Srinivasan, A. F. Westdorp, et al., "EEG coherency. I. Statistics, reference electrode, volume conduction, Laplacians, cortical imaging, and interpretation at multiple scales," *Electroencephalogr. Clini. Neurophysiol.*, **103**, No. 5, 499-515 (1997).

33. G. Nolte, O. Bai, L. Wheaton, et al., "Identifying true brain interaction from EEG data using the imaginary part of coherency," *Clin. Neurophysiol.*, **115**, 2292-2307 (2004).

34. E. Pereda, R. Q. Quiroga, and J. Bhattacharya, "Nonlinear multivariate analysis of neurophysiological signals," *Prog. Neurobiol.*, **77**, Nos. 1/2, 1-37 (2005).

35. A. Sheikhani, H. Behnam, M. R. Mohammadi, et al., "Detection of abnormalities for diagnosing of children with autism disorders using of quantitative electroencephalography analysis," *J. Med. Syst.*, **36**, No. 2, 957-963 (2010).

36. R. Raymaekers, J. R. Wiersema, and H. Roeyers, "EEG study of the mirror neuron system in children with high functioning autism," *Brain Res.*, **1304**, 113-121 (2009).

37. C. Babiloni, F. Babiloni, F. Carducci, et al., "Human cortical electroencephalography (EEG) rhythms during the observation of simple aimless movements: a high-resolution EEG study," *NeuroImage*, **17**, No. 2, 559-572 (2002).

38. J. A. Pineda, B. Z. Allison, A. Vankov, "The effects of self-movement, observation and imagination on mu rhythms and readiness potentials (RP's): toward a brain-computer interface (BCI)," *IEEE Trans. Rehabil. Eng.*, **8**, No. 2, 219-222 (2000).

39. S. Cochin, C. Barthelemy, S. Roux, et al., "Observation and execution of movement: Similarities demonstrated by quantified electroencephalography," *Eur. J. Neurosci.*, **11**, No. 5, 1839-1842 (1999).

40. A. F. Leuchter, S. H. J. Uijtdehaage, I. A. Cook, et al., "Relationship between brain electrical activity and cortical perfusion in normal subjects," *Psychiat. Res.* (*Neuroimaging Sect.*), **90**, 125-140 (1999).

41. I. A. Cook, R. O'Hara, S. H. J. Uijtdehaage, et al., "Assessing the accuracy of topographic EEG mapping for determining local brain function," *Electroencephalogr. Clin. Neurophysiol.*, **107**, No. 6, 408-414 (1998b).

42. I. A. Cook, A. F. Leuchter, M. L. Morgan, et al., "Early changes in prefrontal activity characterize clinical responders to antidepressants," *Neuropsychopharmacology*, **27**, 120-131 (2002).

43. M. Costa, A. L. Goldberger, and C. K. Peng, "Multiscale entropy analysis of complex physiologic time series," *Phys. Rev. Lett.*, **89**, No. 6, 068102 (2002).

44. M. Costa, A. L. Goldberger, and C. K. Peng, "Multiscale entropy analysis of biological signals," *Phys. Rev. E. Stat. Nonlin. Soft. Matter Phys.*, **71**, No. 2, 021906 (2005).

45. J. S. Richman, D. E. Lake, and J. R. Moorman, "Sample entropy analysis," *Methods Enzymol.*, **384**, 172-184 (2004).

46. J. S. Richman and J. R. Moorman, "Physiological time-series analysis using approximate entropy and sample entropy," *Am. J. Physiol. Heart Circ. Physiol.*, **278**, No. 6, 2039-2049 (2000).

47. A. Catarino, O. Churches, S. Baron-Cohen, et al. "Atypical EEG complexity in autism spectrum conditions: A multiscale entropy analysis," *Clin. Neurophysiol.*, **122**, 2375-2383 (2011).

48. A. M. Daoust, E. Limoges, C. Bolduc, et al., "EEG spectral analysis of wakefulness and REM sleep in high functioning autistic spectrum disorders," *Clin. Neurophysiol.*, **115**, 1368-1373 (2004).

49. L. M. Obermana, E. M. Hubband, J. P. Mccleery, et al., "EEG evidence for mirror neuron dysfunction in autism spectrum disorders," *Brain Res. Cogn. Brain Res.*, **24**, No. 2, 190-198 (2005).

50. T. A. Stroganova, G. Nygren, M. M. Tsetlin, et al., "Abnormal EEG lateralization in boys with autism," *Clin. Neurophysiol.*, **118**, 1842-1854 (2007).

51. M. Murias, S. J. Webb, J. Greenson, et al., "Resting state cortical connectivity reflected in EEG coherence in individuals with autism," *Biol. Psychiat.*, **62**, No. 3, 270-273 (2007).

52. R. Bernier, G. Dawson, S. Webb, et al., "EEG mu rhythm and imitation impairments in individuals with autism spectrum disorder," *Brain Cogn.*, **64**, 228-237 (2007).

53. E. V. Orekhova, T. A. Stroganova, G. Nygren, et al., "Excess of high frequency electroencephalogram oscillations in boys with autism," *Biol. Psychiat.*, **62**, 1022-1029 (2007).

54. R. Coben, A. R. Clarke, W. Hudspeth, et al., "EEG power and coherence in autistic spectrum disorder," *Clin. Neurophysiol.*, **119**, 1002-1009 (2008).

55. J. Martineau, S. Cochin, R. Magne, et al., "Impaired cortical activation in autistic children: Is the mirror neuron system involved?" *Int. J. Psychophysiol.*, **68**, 35-40 (2008).

56. V. V. Lazarev, A. Pontes, and L. C. deAzevedo, "EEG photic driving: Right-hemisphere reactivity deficit in childhood autism. A pilot study," *Int. J. Psychophysiol.*, **71**, 177-183 (2009).

57. R. W. Thatcher, D. M. North, J. Neubrander, et al., "Autism and EEG phase reset: deficient GABA mediated inhibition in thalamo-cortical circuits," *Dev. Neuropsychol.*, **34**, No. 6, 780-800 (2009).

58. A. S. Chan, M. C. Cheung, Y. M. Han, et al., "Executive function deficits and neural discordance in children with autism spectrum disorders," *Clin. Neurophysiol.*, **120**, No. 6, 1107-1115 (2009).

59. V. V. Lazarev, A. Pontes, A. A. Mitrofanov, et al., "Interhemispheric asymmetry in EEG photic driving coherence in childhood autism," *Clin. Neurophysiol.*, **121**, 145-152 (2010).

60. S. Sudirman, S. Saidin, and N. M. Safri, "Study of electroencephalography signal of autism and down syndrome children using FFT," in: *Proceedings of the IEEE Symposium on Industrial Electronics and Applications*, Penang (2010), pp. 401-406.

61. J. R. Isler, K. M. Martien, P. G. Grieve, et al., "Reduced functional connectivity in visual evoked potentials in children with autism spectrum disorder," *Clin. Neurophysiol.*, **121**, 2035-2043 (2010).

62. A. S. Chan, Y. M. Y. Han, S. L. Sze, et al., "Disordered connectivity associated with memory deficits in children with autism spectrum disorders," *Res. Autism Spectr. Disord.*, **5**, 237-245 (2011).

63. J. G. Snodgrass and M. Vanderwart, "A standardized set of 260 pictures: Norm for name agreement, image agreement, familiarity, and visual complexity," *J. Exp. Psychol. Hum. Learn.*, **6**, 174-215 (1980).

64. B. Rossion and G. Pourtois, "Revisiting Snodgrass and Vanderwart's object pictorial set: The role of surface detail in basic-level object recognition," *Perception*, **33**, No. 2, 217-236 (2004).

65. E. A. Lushchekina, E. D. Podreznaya, V. S. Lushchekin, et al., "A comparative EEG study in normal and autistic children," *Neurosci. Behav. Physiol.*, **42**, No. 3, 236-243 (2012).

66. K. J. Mathewson, M. K. Jetha, I. E. Drmic, et al., "Regional EEG alpha power, coherence, and behavioral symptomatology in autism spectrum disorder," *Clin. Neurophysiol.*, **123**, No. 9, 1798-1809 (2012).

67. S. Nasehi and H. Pourghassem, "Seizure detection algorithms based on analysis of EEG and ECG signals: A survey," *Neurophysiology*, **44**, 174-186 (2012).

68. A. Sheikhani, H. Behnam, M. R. Mohammadi, et al., "Analysis of quantitative electroencephalogram background activity in autism disease patients with Lempel-Ziv complexity and Short-Time Fourier Transform measure," in: *Proceedings of the 4th IEEE/EMBS, International Summer School and Symposium on Medical Devices and Biosensors. (August 19-22, 2007)*, Cambridge (2007), pp. 19-22.

69. H. Behnam, A. Sheikhani, M. R. Mohammadi, et al., "Abnormalities in connectivity of quantitative electroencephalogram background activity in autism disorders especially in left hemisphere and right temporal," in: *Proceedings of the 10th International Conference on Computer Modeling and Simulation (April 1-3, 2008)*, Cambridge (2008), pp. 82-87.

70. A. Sheikhani, H. Behnam, M. Noroozian, et al., "Abnormalities of quantitative electroencephalography in children with Asperger disorder in various conditions," *Res. Autism Spectr. Disord.*, **3**, 538-546 (2009).

71. M. Ahmadlou, H. Adeli, and A. Adeli, "Fractality and a wavelet-chaos-neural network methodology for EEG-based diagnosis of autistic spectrum disorder," *J. Clin. Neurophysiol.*, **27**, No. 5, 328-333 (2010).

72. N. Razali and A. Wahab, "2D affective space model (ASM) for detecting autistic children," in: *Proceedings of the 15th IEEE International Symposium on Consumer Electronics (June 14-17, 2011)*, Singapore (2011), pp. 536-541.

73. W. Bosl, A. Tierney, H. Tager-Flusberg, et al., "EEG complexity as a biomarker for autism spectrum disorder risk," *BMC Medicine*, **9**, No. 18, (2011).

74. W. K. Shams and A. Wahab, "Characterizing autistic disorder based on principle component analysis," *Austr. J. Basic Appl. Sci.*, **6**, No. 1, 149-155 (2012).

75. F. H. Duffy and H. Als, "A stable pattern of EEG spectral coherence distinguishes children with autism from neurotypical controls – a large case control study," *BMC Med.*, **10**, No. 64 (2012); doi: 10. 1186/1784-7015-10.64.

76. M. J. Alhaddad, M. I. Kamel, H. M. Malibary, et al., "Diagnosis autism by fisher linear discriminant analysis FLDA via EEG," *Int. J. Bio-Sci. Bio-Technol.*, **4**, No. 2 (2012).